Decentralized PD Control for Multi-Robot Collective Transport to a Target Location Using Minimal Information

Hamed Farivarnejad and Spring Berman

Arizona State University, Tempe, AZ, USA

ABSTRACT

In this paper, we propose decentralized position controllers for a team of point-mass robots that must cooperatively transport a payload to a target location. The robots have double-integrator dynamics and are rigidly attached to the payload. The controllers only require robots' measurements of their own positions and velocities, and the only information provided to the robots is the desired position of the payload's center of mass. We consider scenarios in which the robots do not know the position of the payload's center of mass and try to selfishly stabilize their own positions to the desired location, similar to the behaviors exhibited by certain species of ants when retrieving food items in groups. We propose a proportional-derivative (PD) controller that does not rely on inter-robot communication, prior information about the load dynamics and geometry, or knowledge of the number of robots and their distribution around the payload. Using a Lyapunov argument, we prove that under this control strategy, the payload's center of mass converges to a neighborhood of the desired position. Moreover, we prove that the payload's rotation is bounded, and its angular velocity converges to zero. We show that the error between the steady-state position of the payload's center of mass and its desired position depends on the robots' distribution around the payload's center of mass, with a uniform distribution resulting in the lowest steady-state error. We validate our theoretical results with simulations in MATLAB.

Keywords: Collective payload transport, decentralized control, multi-robot systems

1. INTRODUCTION

Potential applications of cooperative payload manipulation by multi-robot systems include construction, manufacturing, assembly in space and underwater, search-and-rescue operations, and disaster response. Many of these scenarios will take place in uncertain environments with unreliable inter-robot communication. In such scenarios, decentralized control strategies that use limited data and communication and have provable guarantees on performance will be needed to reliably achieve manipulation objectives. In this paper, we propose an approach to this problem that is inspired by the phenomenon of group food retrieval in ants 1–3. This behavior is an example of decentralized cooperative manipulation in which the transport teammates do not follow predefined trajectories, use explicit communication, or have prior information about the payload, number and distribution of teammates around it, and locations of obstacles in the environment 4. The specific actions of the ants during collective transport are influenced by their locally perceived information as they navigate back to their nest.

Decentralized control strategies for cooperative manipulation have previously been proposed for scenarios that are not subject to all of these constraints. These strategies, many of which apply to a team of robots with identical sensing and actuation capabilities, are designed to improve the system's robustness to errors, failures, and disturbances. In the decentralized approach proposed in 5, robots push a large payload to a goal when their line of sight to the goal is occluded by the payload. In other approaches, robots communicate their measurements to each other in order to estimate unknown parameters of the payload 6, 7. More recently, 8 proposes an event-triggered communication strategy with distributed impedance control to improve the stability and robustness of cooperative manipulation of unknown payloads in unknown environments. Other approaches do not require inter-robot communication or prior information about the payload dynamics 9, but they rely on a supervisor to

Further author information: (Send correspondence to Spring Berman)
Hamed Farivarnejad: E-mail: hamed.farivarnejad@asu.edu
Spring Berman: E-mail: spring.berman@asu.edu
This work was supported by the Arizona State University Global Security Initiative.

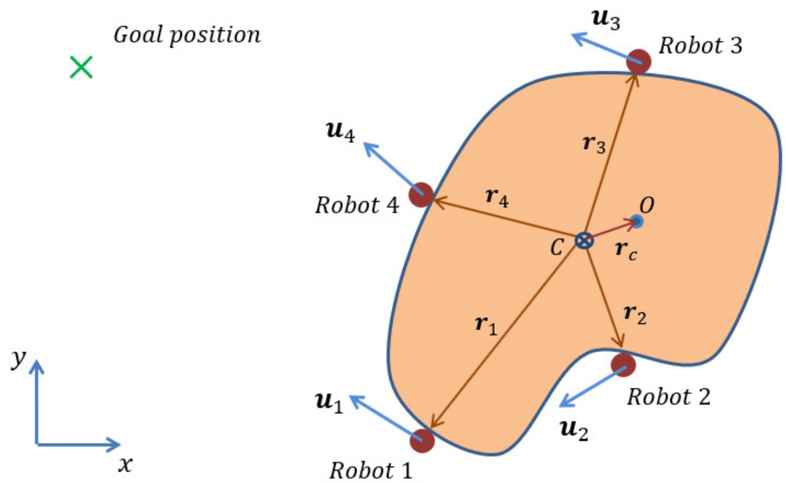

Figure 1: Illustration of a collective transport team with four point-mass robots and the associated coordinate systems.

define the robot and payload trajectories beforehand 10–12. In 13, a strategy inspired by formation control is presented for a flexible payload that requires regulation of contact forces.

Recently, adaptive robust control approaches have been proposed for planar and three-dimensional cooperative manipulation. These approaches combine a stabilizing term with a regression term in the controller in order to achieve stabilization in the presence of parameter uncertainties. However, the approaches require either prior information about the robots' distribution around the payload or feedback on the payload's motion 14–20. In 21, a decentralized approach is proposed for cooperative manipulation in which the robots have a common reference model for the desired payload motion and use an adaptive controller to compensate for the effect of friction on the payload. Whereas this approach requires the robots to have access to measurements of the payload's linear and angular velocities, ours does not require any information on the payload's motion.

Recently, learning schemes have also been proposed for cooperative manipulation. In 22, robots in a transport team, which explicitly exchange information, jointly reach the same desired motion by running a time-varying quadratic program which is solved online by a neural network scheme. A dynamic recurrent neural network is used in 23 to solve a quadratic program, which computes cooperative kinematic controllers for redundant manipulators using partially known information about the payload and the teammates. In addition, reinforcement learning is used in 24 to design two distributed approaches to cooperative manipulation: the first applies Q-learning with individual reward functions, and the second utilizes game-theoretic techniques. The first approach exhibits more robustness to different reward structures than the second.

In this paper, we design decentralized position controllers for a collective transport task by a group of point-mass robots that lack inter-robot communication and can only use on-board measurements of their own positions and velocities as feedback. The controllers have a proportional-derivative (PD) structure and drive the robots to transport the payload to a target destination. In our prior work 25, we addressed the problem of controlling the velocity of the payload, rather than its position, for a multi-robot transport team subject to these constraints. We analytically prove asymptotic convergence of the payload's center of mass to a neighborhood of the target position and study the parameters that influence the steady-state distance between the payload's center of mass and this goal position. We validate our control approach with numerical simulations.

2. PROBLEM STATEMENT

We consider a team of N identical point-mass robots that move on a planar surface and are rigidly attached to a payload in an arbitrary configuration, as shown in Fig. 1. We assume that each robot has access to its own position and velocity with respect to an inertial coordinate system, which is common to all the robots. The robots do not communicate with one another and are not assigned predefined trajectories. They also lack

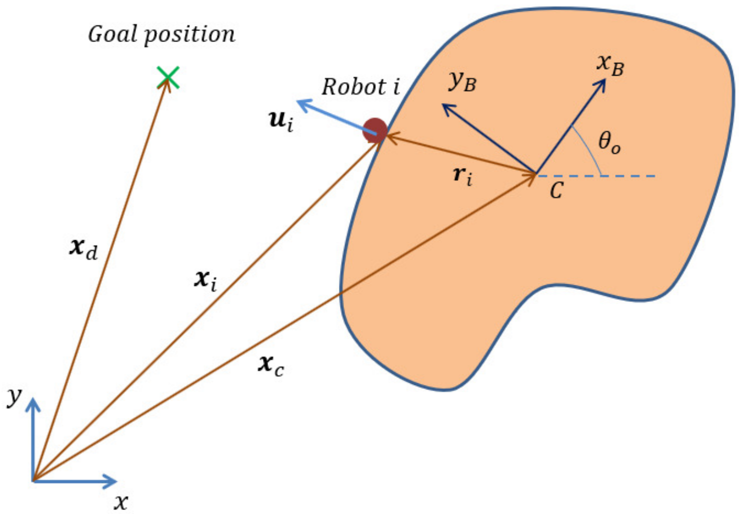

Figure 2: Illustration of the geometric parameters that express the position of a robot in the local coordinate frame of the load.

information about the payload's kinematics and dynamics, the number of robots in the transport team, and the robots' distribution around the payload.

We define $\boldsymbol{x}_o = [x_o \ y_o]^T \in \mathbb{R}^2$ and $\theta_o \in \mathbb{R}$ as the position of the payload's center of mass, point O in Fig. 1, and the payload's orientation with respect to a global coordinate frame, respectively. We define $\boldsymbol{x}_i = [x_i \ y_i]^T \in \mathbb{R}^2$ as the position of robot i and $\boldsymbol{x}_d = [x_d \ y_d]^T \in \mathbb{R}^2$ as the position of the target point in the global frame, as shown in Fig. 2. The center of mass of the entire system, including both the load and the robots, is denoted by point C in Fig. 1. Given that points O and C are not necessarily coincident, we define $\boldsymbol{x}_c = [x_c \ y_c]^T \in \mathbb{R}^2$ as the position of C in the global frame and $\mathbf{r}_c \in \mathbb{R}^2$ as the vector from C to O, as shown in Fig. 1. We also define $\boldsymbol{r}_i = [r_{ix} \ r_{iy}]^T \in \mathbb{R}^2$ as the vector from C to the attachment point of robot i in the global frame.

Each robot i knows its own position $\boldsymbol{x}_i$ and velocity $\dot{\boldsymbol{x}}_i$ and applies an actuating force $\boldsymbol{u}_i = [u_{ix} \ u_{iy}]^T \in \mathbb{R}^2$ to the payload. The control objective is to design the forces $\boldsymbol{u}_i$, $i = 1, ..., N$, such that the robots drive the position of the payload's center of mass, $\boldsymbol{x}_o$, to the target position $\boldsymbol{x}_d$. The only sensor feedback available to the robots consists of their on-board measurements of their own positions and velocities.

3. DYNAMICAL MODEL

To derive the dynamical model of the entire system, comprised of both the load and the robots, we use the framework in our previous papers 25, 26. We denote the mass of each robot and the mass of the payload by m_r and m_o, respectively. We also define I_o as the payload's moment of inertia about the axis perpendicular to the plane and passing through O. Considering the entire system as a rigid body and defining $\boldsymbol{q} := [x_c \ y_c \ \theta_o]^T \in \mathbb{R}^3$ as the vector of generalized coordinates, we can write the equation of motion of the entire system as

$$\begin{bmatrix} m\boldsymbol{I} & 0 \\ 0 & I \end{bmatrix} \ddot{\boldsymbol{q}} = \begin{bmatrix} \boldsymbol{I} & \cdots & \boldsymbol{I} \\ \hat{\boldsymbol{r}}_1^T & \dots & \hat{\boldsymbol{r}}_N^T \end{bmatrix} \boldsymbol{u}, \tag{1}$$

where m and I are the mass and moment of inertia of the entire system, given by:

$$\begin{aligned} m &= m_o + N m_r, \\ I &= I_o + m_o \left\|\mathbf{r}_c\right\|^2 + m_r \sum_{i=1}^{N} \left\|\mathbf{r}_i\right\|^2, \end{aligned} \tag{2}$$

and $\hat{\boldsymbol{r}}_i \in \mathbb{R}^2$ and $\boldsymbol{u} \in \mathbb{R}^{2N}$ are defined as

$$\hat{\boldsymbol{r}}_i = [-r_{iy} \;\; r_{ix}]^T, \tag{3}$$
$$\boldsymbol{u} = [\boldsymbol{u}_1^T \;\cdots\; \boldsymbol{u}_N^T]^T. \tag{4}$$

The matrix $\boldsymbol{I} \in \mathbb{R}^{2\times 2}$ is the identity matrix.

4. CONTROLLER DESIGN

In this section, we present decentralized robot controllers for the system described by Eq. 1 that produce asymptotic convergence of the payload's center of mass to a neighborhood of the desired position $\boldsymbol{x}_d$. The proposed control law has a proportional-derivative (PD) structure,

$$\boldsymbol{u}_i = -\boldsymbol{K}_d \dot{\boldsymbol{x}}_i - \boldsymbol{K}_p(\boldsymbol{x}_i - \boldsymbol{x}_d), \tag{5}$$

in which $\boldsymbol{K}_p = K_p\boldsymbol{I}$ and $\boldsymbol{K}_d = K_d\boldsymbol{I}$ are gain matrices, where K_p and K_d are strictly positive constants. This control law implies that each robot *selfishly* tries to stabilize its own position to the target position. Since the robots are attached to distinct points on the payload's boundary, convergence of all the robots' positions to the target position is impossible. However, by each applying the decentralized controller in Eq. 5, the robots produce a collective transport behavior that approximately achieves the control objective defined in Section 2. We analyze and discuss this behavior in the next section.

5. MOTION ANALYSIS

To analyze the collective behavior of the entire system of the payload and robots with the proposed controller, we first derive the dynamics of the closed-loop system and then investigate the stability and convergence properties of this system.

5.1 Closed-Loop Dynamics

There is a holonomic kinematic constraint between the position of robot i and the position of the system's center of mass (see Fig. 2), given by

$$\boldsymbol{x}_i = \boldsymbol{x}_c + \boldsymbol{r}_i. \tag{6}$$

Taking the time derivative of Eq. 6, we obtain

$$\dot{\boldsymbol{x}}_i = \dot{\boldsymbol{x}}_c + \hat{\boldsymbol{r}}_i \dot{\theta}_o, \tag{7}$$

where $\hat{\boldsymbol{r}}_i$ is given by Eq. 3. We define $\boldsymbol{e}_c := \boldsymbol{x}_c - \boldsymbol{x}_d$, where $\dot{\boldsymbol{e}}_c = \dot{\boldsymbol{x}}_c$ and $\ddot{\boldsymbol{e}}_c = \ddot{\boldsymbol{x}}_c$, since $\boldsymbol{x}_d$ is constant. Substituting the expressions for $\boldsymbol{x}_i$ and $\dot{\boldsymbol{x}}_i$ in Eqs. 6 and 7 into Eq. 5, we obtain

$$\boldsymbol{u}_i = -\boldsymbol{K}_d(\dot{\boldsymbol{e}}_c + \hat{\boldsymbol{r}}_i\dot{\theta}_o) - \boldsymbol{K}_p(\boldsymbol{e}_c + \boldsymbol{r}_i). \tag{8}$$

We now incorporate the decentralized control law for $\boldsymbol{u}_i$ in Eq. 8 into the dynamical model in Eq. 1 to derive the equation of motion of the closed-loop system as

$$\begin{aligned}\boldsymbol{M}\ddot{\boldsymbol{e}}_c &= -\boldsymbol{K}_d\sum_{i=1}^{N}(\dot{\boldsymbol{e}}_c + \hat{\boldsymbol{r}}_i\dot{\theta}_o) - \boldsymbol{K}_p\sum_{i=1}^{N}(\boldsymbol{e}_c + \boldsymbol{r}_i),\\ I\ddot{\theta}_o &= -K_d\sum_{i=1}^{N}\hat{\boldsymbol{r}}_i^T(\dot{\boldsymbol{e}}_c + \hat{\boldsymbol{r}}_i\dot{\theta}_o) - K_p\sum_{i=1}^{N}\hat{\boldsymbol{r}}_i^T(\boldsymbol{e}_c + \boldsymbol{r}_i),\end{aligned} \tag{9}$$

where $\boldsymbol{M} = m\boldsymbol{I}$. Taking into account the facts that $\boldsymbol{r}_i \times \boldsymbol{r}_i = \boldsymbol{0}$ and $[\boldsymbol{r}_i^T\ 0]^T \times [\boldsymbol{a}^T\ 0]^T = [0\ \ 0\ \ \hat{\boldsymbol{r}}_i^T \boldsymbol{a}]^T$, where $\boldsymbol{a}$ is an arbitrary vector in $\mathbb{R}^2$, the closed-loop system in Eq. 9 can be rewritten as

$$
\begin{aligned}
\boldsymbol{M}\ddot{\boldsymbol{e}}_c &= -N\boldsymbol{K}_d\dot{\boldsymbol{e}}_c - \boldsymbol{K}_d\sum_{i=1}^{N}\hat{\boldsymbol{r}}_i\,\dot{\theta}_o - N\boldsymbol{K}_p\boldsymbol{e}_c - \boldsymbol{K}_p\sum_{i=1}^{N}\boldsymbol{r}_i,\\
I\ddot{\theta}_o &= -K_d\sum_{i=1}^{N}\hat{\boldsymbol{r}}_i^T\dot{\boldsymbol{e}}_c - K_d\sum_{i=1}^{N}\|\boldsymbol{r}_i\|^2\,\dot{\theta}_o - K_p\sum_{i=1}^{N}\hat{\boldsymbol{r}}_i^T\boldsymbol{e}_c.
\end{aligned}
\tag{10}
$$

For notational simplicity, we define $\boldsymbol{\varrho} := \sum_{i=1}^{N}\boldsymbol{r}_i$, which implies that $\hat{\boldsymbol{\varrho}} := \sum_{i=1}^{N}\hat{\boldsymbol{r}}_i$, and $\rho := \sum_{i=1}^{N}\|\boldsymbol{r}_i\|^2$. Note that while the direction of $\boldsymbol{\varrho}$ changes with the payload's rotation, its magnitude remains unchanged since the robots are rigidly attached to the payload and C is a fixed point on the payload.

5.2 Convergence Analysis

The equilibrium state of the closed-loop system in Eq. 10 is obtained by setting $\ddot{\boldsymbol{e}}_c = \dot{\boldsymbol{e}}_c = \boldsymbol{0}$ and $\ddot{\theta}_o = \dot{\theta}_o = 0$, which results in the following equations:

$$
N\boldsymbol{e}_c^* + \boldsymbol{\varrho}^* = \boldsymbol{0}, \tag{11}
$$

$$
\left(\hat{\boldsymbol{\varrho}}^*\right)^T\boldsymbol{e}_c^* = 0, \tag{12}
$$

in which the superscript * denotes the equilibrium state. Solving Eq. 11 for $\boldsymbol{e}_c^*$, we obtain $\boldsymbol{e}_c^* = -\frac{1}{N}\boldsymbol{\varrho}^*$. Since $\hat{\boldsymbol{\varrho}}$ is perpendicular to $\boldsymbol{\varrho}$ by definition, this shows that Eq. 12 is redundant. Also, since $\boldsymbol{\varrho}$ has a constant norm, the steady-state error $\boldsymbol{e}_c^*$ has a constant magnitude. The set of equilibrium states $\mathcal{E}$ is therefore obtained as

$$
\mathcal{E} = \left\{\boldsymbol{e}_c, \dot{\boldsymbol{e}}_c \in \mathbb{R}^2,\, \theta_o, \dot{\theta}_o \in \mathbb{R}\ \middle|\ \boldsymbol{e}_c = -\frac{1}{N}\boldsymbol{\varrho},\, \dot{\boldsymbol{e}}_c = \boldsymbol{0},\, \dot{\theta}_o = 0\right\}. \tag{13}
$$

Note that the payload's orientation θ_o is not specified in $\mathcal{E}$, which means that $\mathcal{E}$ is a manifold in the state space and not an isolated equilibrium point. To analyze the convergence of the closed-loop system's trajectories to $\mathcal{E}$, we consider the following quadratic positive semidefinite function,

$$
V = \frac{1}{2}\dot{\boldsymbol{e}}_c^T\boldsymbol{M}\dot{\boldsymbol{e}}_c + \frac{1}{2}I\dot{\theta}_o^2 + \frac{1}{2N}(N\boldsymbol{e}_c + \boldsymbol{\varrho})^T\boldsymbol{K}_p(N\boldsymbol{e}_c + \boldsymbol{\varrho}), \tag{14}
$$

which is zero in the set $\mathcal{E}$ and positive everywhere else. The time derivative of V is calculated as

$$
\begin{aligned}
\dot{V} = &\ \dot{\boldsymbol{e}}_c^T\boldsymbol{M}\ddot{\boldsymbol{e}}_c + I\dot{\theta}_o\ddot{\theta}_o + \frac{1}{N}(N\boldsymbol{e}_c + \boldsymbol{\varrho})^T\boldsymbol{K}_p(N\dot{\boldsymbol{e}}_c + \dot{\boldsymbol{\varrho}})\\
= &\ \dot{\boldsymbol{e}}_c^T(-N\boldsymbol{K}_d\dot{\boldsymbol{e}}_c - \boldsymbol{K}_d\hat{\boldsymbol{\varrho}}\,\dot{\theta}_o - N\boldsymbol{K}_p\boldsymbol{e}_c - \boldsymbol{K}_p\boldsymbol{\varrho}) + \dot{\theta}_o(-K_d\hat{\boldsymbol{\varrho}}^T\dot{\boldsymbol{e}}_c - K_d\rho\dot{\theta}_o - K_p\hat{\boldsymbol{\varrho}}^T\boldsymbol{e}_c)\\
&+ N\boldsymbol{e}_c^T\boldsymbol{K}_p\dot{\boldsymbol{e}}_c + \boldsymbol{e}_c^T\boldsymbol{K}_p\dot{\boldsymbol{\varrho}} + \boldsymbol{\varrho}^T\boldsymbol{K}_p\dot{\boldsymbol{e}}_c + \frac{1}{N}\boldsymbol{\varrho}^T\boldsymbol{K}_p\dot{\boldsymbol{\varrho}}.
\end{aligned}
\tag{15}
$$

We see that many terms in the above expression cancel out. Moreover, since we can confirm that $\dot{\boldsymbol{\varrho}} = -\hat{\boldsymbol{\varrho}}\dot{\theta}_o$ and $\boldsymbol{\varrho}^T\hat{\boldsymbol{\varrho}} = 0$, the last term in the right-hand side of Eq. 15 is zero. Hence, $\dot{V}$ is simplified to

$$
\dot{V} = -N\dot{\boldsymbol{e}}_c^T\boldsymbol{K}_d\dot{\boldsymbol{e}}_c - NK_d\rho\dot{\theta}_o^2 - \dot{\boldsymbol{e}}_c^T\boldsymbol{K}_d\hat{\boldsymbol{\varrho}}\dot{\theta}_o - \dot{\theta}_oK_d\hat{\boldsymbol{\varrho}}^T\dot{\boldsymbol{e}}_c, \tag{16}
$$

which can be rewritten in the following quadratic form:

$$
\dot{V} = -\begin{bmatrix}\dot{\boldsymbol{e}}_c^T & \dot{\theta}_o\end{bmatrix}\underbrace{\begin{bmatrix}N\boldsymbol{K}_d & \boldsymbol{K}_d\hat{\boldsymbol{\varrho}}\\ K_d\hat{\boldsymbol{\varrho}}^T & NK_d\rho\end{bmatrix}}_{\boldsymbol{Q}}\begin{bmatrix}\dot{\boldsymbol{e}}_c\\ \dot{\theta}_o\end{bmatrix}. \tag{17}
$$

The matrix $\boldsymbol{Q} \in \mathbb{R}^{3\times 3}$ is the same matrix $\boldsymbol{Q}$ in our previous work [25, Theorem 3.1, Eq. (12)], which we proved is positive definite. This shows that $\dot{V}$ is negative semidefinite, and henceforth V remains bounded throughout the motion of the entire system. Furthermore, invoking *LaSalle's invariant principle*, we can conclude that the trajectories of the closed-loop system in Eq. 10 converge to a set that is characterized by $\dot{V} \equiv 0$, for which $\dot{\boldsymbol{e}}_c \equiv \mathbf{0}$ and $\dot{\theta}_o \equiv 0$. This is the set $\mathcal{E}$ in Eq. 13. Convergence of the closed-loop system's trajectories to $\mathcal{E}$ implies that as $t \to \infty$, the center of mass of the entire system (C) converges to a neighborhood of the target position $\boldsymbol{x}_d$ and the payload's angular velocity $\dot{\theta}_o$ converges to zero. The uniform continuity of θ_o implies the convergence of θ_o to a bounded value, which depends on its initial value.

To analyze the convergence of the payload's center of mass (O) to the target position, we define $\boldsymbol{r}_{i,o}$ as the vector from point O to robot i and $\boldsymbol{\varrho}_o := \sum_{i=1}^{N} \boldsymbol{r}_{i,o}$. We also define $\boldsymbol{e}_o = \boldsymbol{x}_o - \boldsymbol{x}_d$. We can confirm that for a group of robots attached rigidly to a payload,

$$\boldsymbol{r}_c = -\frac{m_r}{m_o}\boldsymbol{\varrho} = -\frac{m_r}{m}\boldsymbol{\varrho}_o. \tag{18}$$

Moreover, since $\boldsymbol{x}_c = \boldsymbol{x}_o - \boldsymbol{r}_c$, we can write

$$\boldsymbol{e}_c = \boldsymbol{e}_o - \boldsymbol{r}_c. \tag{19}$$

Substituting Eq. 18 for $\boldsymbol{r}_c$ into Eq. 19 and then incorporating the result into Eq. 11, we obtain

$$\boldsymbol{e}_o^* = -\frac{1}{N}\boldsymbol{\varrho}_o^*, \tag{20}$$

which gives the position error of the payload's center of mass at equilibrium. Like $\boldsymbol{\varrho}$, $\boldsymbol{\varrho}_o$ has a constant magnitude, since the robots are rigidly attached to the payload and O is a fixed point on the payload. Eq. 20 shows that the steady-state distance between the payload's center of mass and the target position depends on the number of robots N and their distribution around the payload. This distance decreases as N is increased, and for payloads with a homogeneous mass density, it decreases as the distribution of robots around the payload's center of mass approaches a uniform distribution. For non-homogeneous payloads, this distance is reduced by allocating the robots in accordance with the payload's mass distribution; e.g., increasing the number of robots around sections of the payload with high mass density. The direction of $\boldsymbol{e}_o^*$ depends on the steady-state value of the payload orientation θ_o through $\boldsymbol{\varrho}_o^*$; the steady-state orientation depends on the initial value of θ_o, as stated earlier.

6. SIMULATION RESULTS

We validate our analysis with simulation results for collective transport by a team of identical robots that are arranged in three different distributions around a circular payload. For each simulation, we observe the time evolution of the payload's orientation, angular velocity, and the position and velocity of its center of mass. We also study the effect of the robot distribution on the steady-state error of the payload's center of mass with respect to the target position.

The load is modeled as a homogeneous circular ring with mass $m_o = 1$ kg and moment of inertia $I_o = 0.33$ kg·m^2. Six point-mass robots, each with mass $m_r = 0.05$ kg, are rigidly attached to the load. The controller gain are $K_p = 0.8$ and $K_v = 0.3$. The payload's center of mass is initially located at $\boldsymbol{x}_o(t=0) = [3 \ \ -1.5]^T$ m. The simulations were each run for 40 s.

Figs. 3-5 show snapshots of the payload over time for each robot distribution. The robot locations are marked as red points on the perimeter of the load in its initial and final configurations. The target position is shown as a green star at the origin, and the actual trajectory of the payload's center of mass is plotted in dashed green. The red dashed line on the load indicates its orientation. The gray circles and the orange dashed lines on them show the payload and its orientation, respectively, in intermediate states. In addition, Figs. 6-7 show the time evolution of the position and velocity of the payload's center of mass for the three distributions. Also, Fig. 8 plots the corresponding time evolution of the load's angular position and velocity.

In the first simulation (Fig. 3), the robots have an equally-spaced distribution, and the load is transported to the target position with zero steady-state error. This happens because $||\boldsymbol{\varrho}_o|| = 0$, which results in Eq. 20 yielding $||\boldsymbol{e}_o^*|| = 0$. The position and velocity of the payload's center of mass converge to zero quickly after around 7 s (the blue lines in Figs. 6 and 7). Also, the payload shows zero rotation and angular velocity during the entire transport (the blue lines in Fig. 8). In the second simulation (Fig. 4), the robots have a nonuniform

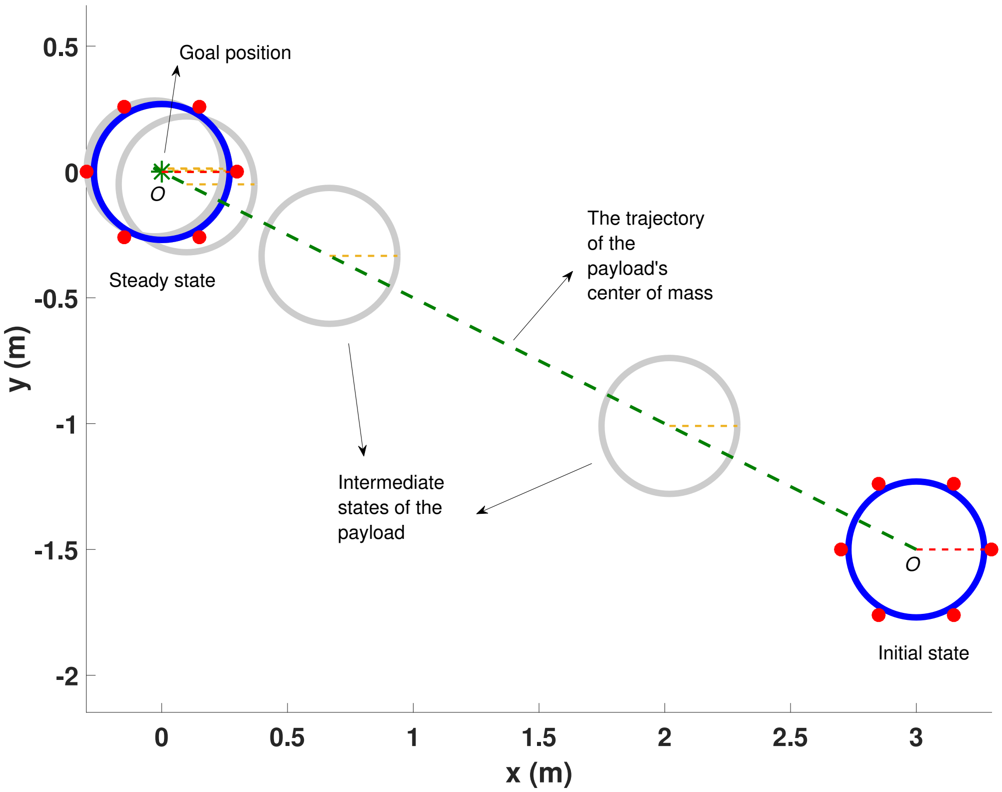

Figure 3: Snapshots of the payload over time with an equally-spaced distribution of robots around its perimeter (Distribution 1).

distribution for which $||\boldsymbol{\varrho}_o|| = 1.058$ m. Using Eq. 20, we can obtain $||\boldsymbol{e}_o^*|| = 0.176$ m. The position and velocity of the payload's center of mass converge to their steady-state values after around 10 s (the orange lines in Figs. 6 and 7), which is a little slower than in the first simulation. In addition, the load undergoes a total rotation of approximately $\theta_o = 85°$ (the orange lines in Fig. 8). In the third simulation (Fig. 5), the robots are clustered within about a quarter of the load's perimeter. For this case, $||\boldsymbol{\varrho}_o|| = 1.477$ m, and the steady-state error has increased to $||\boldsymbol{e}_o^*|| = 0.246$ m. We also see that the system convergence to equilibrium is much slower than in the first and second simulations. The payload's position and velocity converge to their steady-state values after about 25 s (the green lines in Figs. 6 and 7). The load undergoes a large rotation of about $\theta_o = 248°$, and its angular velocity converges to zero after around 35 s (the green lines in Fig. 8). Thus, a highly nonuniform distribution of robots significantly affects the system's steady-state error and convergence characteristics.

7. CONCLUSION

We have proposed a decentralized PD control strategy for a team of identical point-mass robots to collectively transport a payload to a target position. The controller only requires the robots' local measurements and does not rely on predefined trajectories and explicit communication between the robots. We proved that with the proposed controller, the robots drive the payload to a neighborhood of the destination, where the steady-state distance between the payload's center of mass and the target position is only a function of the number of the robots and their distribution around the payload. In ongoing work, we are considering environments with convex obstacles and modifying the controller to enable the robots to transport the payload to the destination while avoiding collisions with the obstacles.

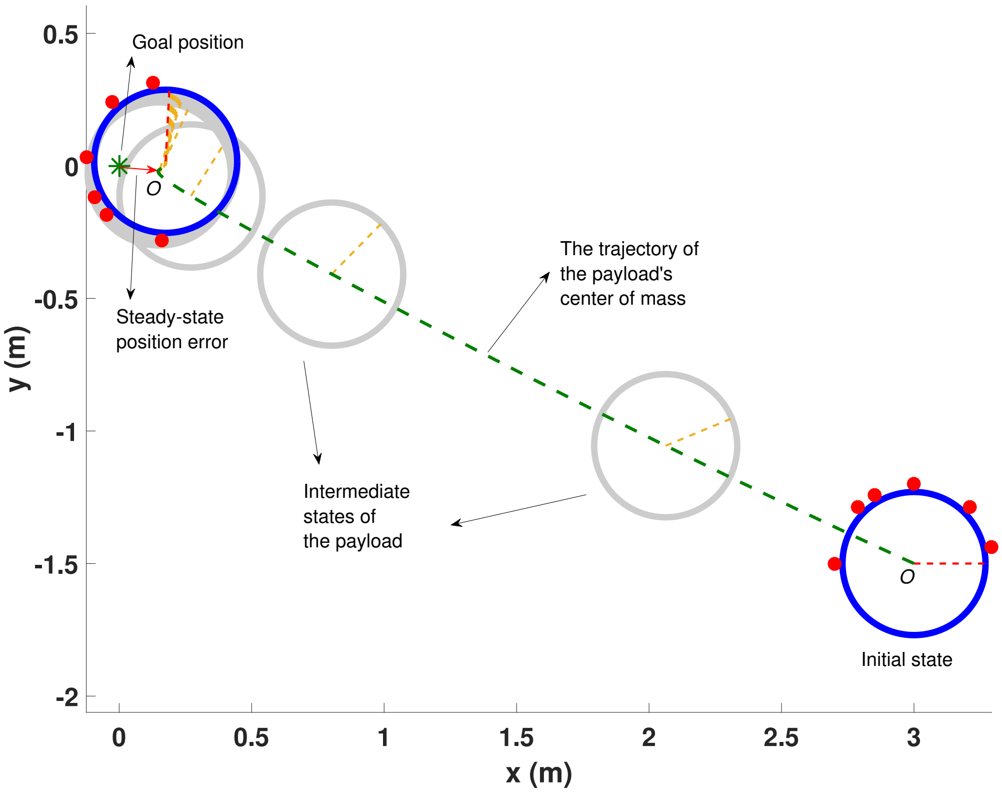

Figure 4: Snapshots of the payload over time with a nonuniform distribution of robots around its perimeter (Distribution 2).

REFERENCES

[1] Czaczkes, T. J. and Ratnieks, F. L., "Cooperative transport in ants (Hymenoptera: Formicidae) and elsewhere," *Myrmecological News* **18**, 1–11 (2013).

[2] McCreery, H. F. and Breed, M., "Cooperative transport in ants: a review of proximate mechanisms," *Insectes Sociaux* **61**(2), 99–110 (2014).

[3] Gelblum, A., Pinkoviezky, I., Fonio, E., Gov, N. S., and Feinerman, O., "Emergent oscillations assist obstacle negotiation during ant cooperative transport," *Proceedings of the National Academy of Sciences* **113**(51), 14615–14620 (2016).

[4] Medina, O., Hacohen, S., and Shvalb, N., "Robotic swarm motion planning for load carrying and manipulating," *IEEE Access* **8**, 53141–53150 (2020).

[5] Chen, J., Gauci, M., Li, W., Kolling, A., and Groß, R., "Occlusion-based cooperative transport with a swarm of miniature mobile robots," *IEEE Transactions on Robotics* **31**(2), 307–321 (2015).

[6] Franchi, A., Petitti, A., and Rizzo, A., "Distributed estimation of the inertial parameters of an unknown load via multi-robot manipulation," in [*Proc. IEEE Int'l. Conf. on Decision and Control*], 6111–6116 (Dec 2014).

[7] Marino, A., Muscio, G., and Pierri, F., "Distributed cooperative object parameter estimation and manipulation without explicit communication," in [*Proc. IEEE Int'l. Conf. on Robotics and Automation (ICRA)*], 2110–2116 (May 2017).

[8] Dohmann, P. B. G. and Hirche, S., "Distributed control for cooperative manipulation with event-triggered communication," *IEEE Transactions on Robotics* (2020).

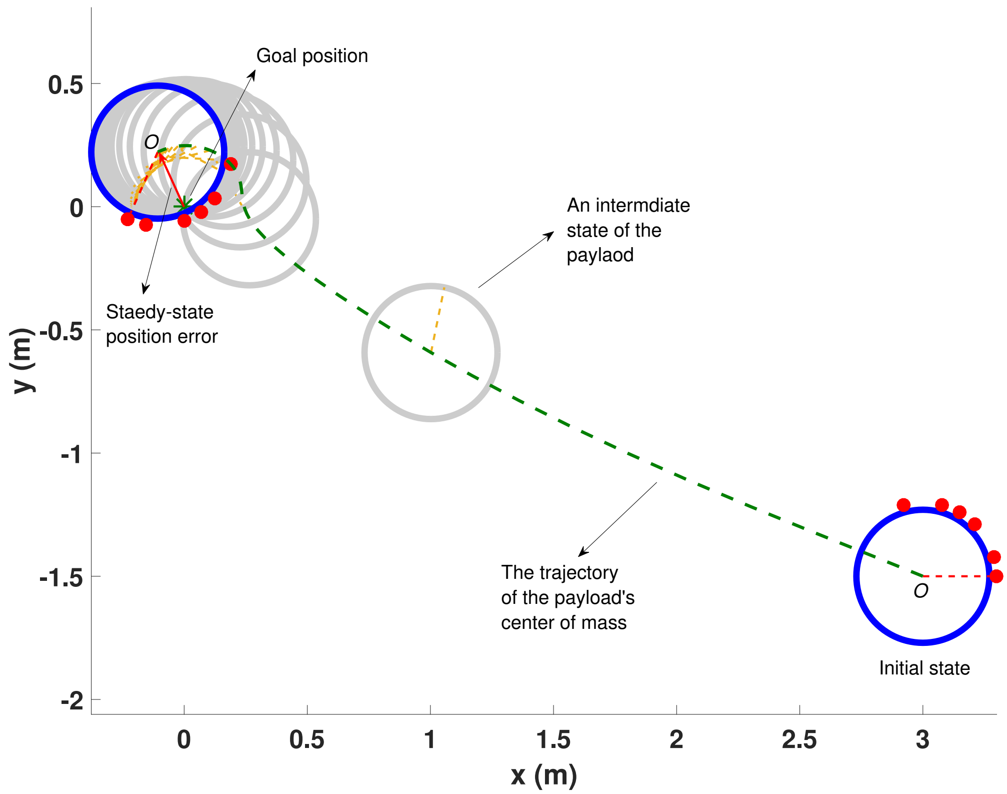

Figure 5: Snapshots of the payload over time with a highly nonuniform distribution of robots around its perimeter (Distribution 3).

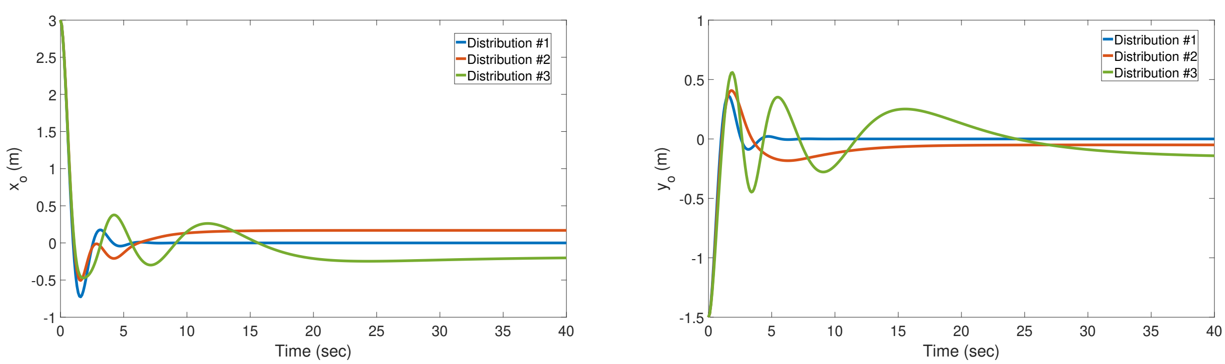

(a) Position component along the x-axis.

(b) Position component along the y-axis.

Figure 6: Time evolution of the position of the payload's center of mass for the three distributions.

[9] Marino, A. and Pierri, F., "A two stage approach for distributed cooperative manipulation of an unknown object without explicit communication and unknown number of robots," *Robotics and Autonomous Systems* **103**, 122 – 133 (2018).

[10] Tsiamis, A., Verginis, C. K., Bechlioulis, C. P., and Kyriakopoulos, K. J., "Cooperative manipulation exploiting only implicit communication," in [*Proc. IEEE/RSJ Int'l. Conf. on Intelligent Robots and Systems (IROS)*], 864–869 (Sept 2015).

[11] Gueaieb, W., Karray, F., and Al-Sharhan, S., "A robust adaptive fuzzy position/force control scheme for

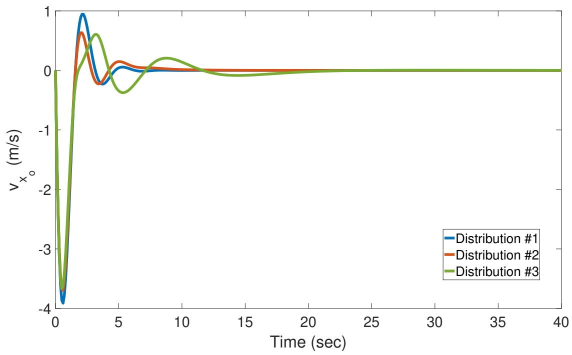

(a) Velocity component along the x-axis.

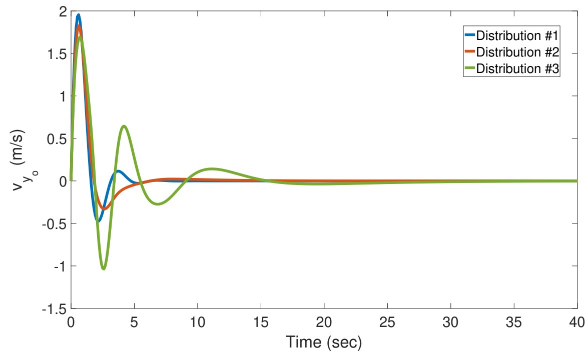

(b) Velocity component along the y-axis.

Figure 7: Time evolution of the velocity of the payload's center of mass for the three distributions.

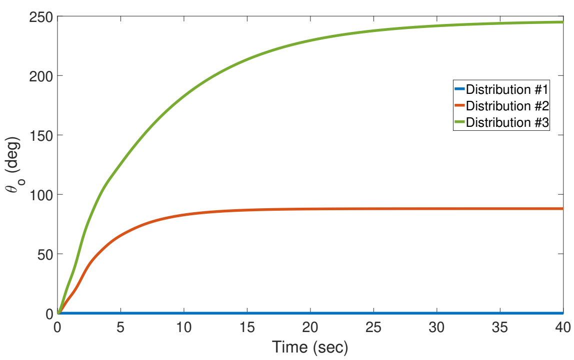

(a) Angular position.

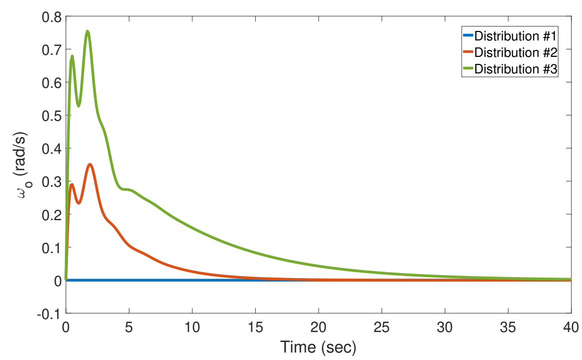

(b) Angular velocity.

Figure 8: Time evolution of the rotational motion of the payload for the three distributions.

cooperative manipulators," *IEEE Transactions on Control Systems Technology* **11**, 516–528 (July 2003).

[12] Li, Z., Yang, C., Su, C. Y., Deng, S., Sun, F., and Zhang, W., "Decentralized fuzzy control of multiple cooperating robotic manipulators with impedance interaction," *IEEE Transactions on Fuzzy Systems* **23**, 1044–1056 (Aug 2015).

[13] Bai, H. and Wen, J. T., "Cooperative load transport: A formation-control perspective," *IEEE Transactions on Robotics* **26**, 742–750 (Aug 2010).

[14] Kim, S., Seo, H., Shin, J., and Kim, H. J., "Cooperative aerial manipulation using multirotors with multi-dof robotic arms," *IEEE/ASME Transactions on Mechatronics* **23**(2), 702–713 (2018).

[15] Lee, H., Kim, H., Kim, W., and Kim, H. J., "An integrated framework for cooperative aerial manipulators in unknown environments," *IEEE Robotics and Automation Letters* **3**(3), 2307–2314 (2018).

[16] Sadati, N. and Ghaffarkhah, A., "Decentralized position and force control of nonredundant multi-manipulator systems," in [*Proc. Int'l. Conf. on Control, Automation and Systems*], 2223–2229 (Oct 2007).

[17] Dai, G. B. and Liu, Y. C., "Distributed coordination and cooperation control for networked mobile manipulators," *IEEE Transactions on Industrial Electronics* **64**, 5065–5074 (June 2017).

[18] Lee, H., Kim, H., and Kim, H. J., "Planning and control for collision-free cooperative aerial transportation," *IEEE Transactions on Automation Science and Engineering* **15**(1), 189–201 (2016).

[19] Marino, A., "Distributed adaptive control of networked cooperative mobile manipulators," *IEEE Transactions on Control Systems Technology* **26**(5), 1646–1660 (2017).

[20] Pliego-Jimenez, J. and Arteaga-Perez, M., "On the adaptive control of cooperative robots with time-variant holonomic constraints," *International Journal of Adaptive Control and Signal Processing* **31**(8), 1217–1231 (2017).

[21] Culbertson, P. and Schwager, M., "Decentralized adaptive control for collaborative manipulation," in [*Proc. IEEE Int'l. Conf. on Robotics and Automation (ICRA)*], 278–285 (May 2018).

[22] Jin, L., Li, S., Luo, X., Li, Y., and Qin, B., "Neural dynamics for cooperative control of redundant robot manipulators," *IEEE Transactions on Industrial Informatics* **14**(9), 3812–3821 (2018).

[23] Li, X., Xu, Z., Li, S., Wu, H., and Zhou, X., "Cooperative kinematic control for multiple redundant manipulators under partially known information using recurrent neural network," *IEEE Access* **8**, 40029–40038 (2020).

[24] Ding, G., Koh, J. J., Merckaert, K., Vanderborght, B., Nicotra, M. M., Heckman, C., Roncone, A., and Chen, L., "Distributed reinforcement learning for cooperative multi-robot object manipulation," *arXiv preprint arXiv:2003.09540* (2020).

[25] Farivarnejad, H. and Berman, S., "Stability and convergence analysis of a decentralized proportional-integral control strategy for collective transport," in [*Proc. American Control Conference (ACC)*], 2794–2801 (June 2018).

[26] Farivarnejad, H., Wilson, S., and Berman, S., "Decentralized sliding mode control for autonomous collective transport by multi-robot systems," in [*2016 IEEE 55th Conference on Decision and Control (CDC)*], 1826–1833 (Dec 2016).